PROCEEDINGS of ISMA 2019
International Symposium on Music Acoustics

13 - 17 September 2019 in Detmold, Germany

Measurement and modeling of a resonator guitar

Mark Rau[(1)]*, Julius O. Smith III[(1)]

[(1)]Center for Computer Research in Music and Acoustics, Stanford University, USA

Abstract

Resonator guitars are acoustic instruments which have one or more spun metal cones embedded in the top plate, with strings driving the cone directly through a bridge. They were originally designed to be louder than traditional acoustic guitars and are often played with a metal slide. The vibrational characteristics of resonator guitars having a single inverted-cone are studied as the basis for a synthesis model. The small-signal input admittance is obtained using an impact hammer and laser Doppler vibrometer. As well, sinusoidal sweeps are made using a modal shaker at various driving amplitude levels. The shaker measurements show that some of the modes exhibit nonlinear characteristics. These measurements are used to design body resonator filters with time-varying resonant modes for a digital waveguide model of the resonator guitar.

Keywords: Guitar, Measurement, Modeling

1 INTRODUCTION

During the early twentieth century, the playing levels of American bands were increasing due to the use of brass instruments and percussion. Conventional stringed instruments were not loud enough to compete, leading to the invention of “resophonic” or “resonator” instruments. Resonator instruments have similar construction to their traditional counterparts, with the addition of one or more spun metal cones replacing the majority of the top plates. With the introduction of electronically amplified musical instruments, the need for louder acoustic instruments was reduced, but by this time, resophonic instruments had already become part of the canon of American music such as blues and traditional music. While there are resophonic versions of many instruments such as banjos, mandolins, and ukuleles, by far the most popular variant is that of the guitar.

There are three main styles of resonator cone instruments: the single-cone “biscuit”, single inverted cone, and tricone designs [1]. The biscuit design uses a large cone having an approximately 24 cm diameter, mounted flush with the instrument’s top plate, with the bridge mounted at the peak of the cone. The inverted cone design uses a similar cone, but with it being inverted, and a small protrusion where the bridge is mounted. Tricone resonators use three smaller cones, typically of the biscuit style, with the bridge mounted to a metal structure connecting the peaks of each cone.

In addition to the different cone styles, there are two different neck setups commonly found on resonator guitars. Some resonator guitars have a standard round neck and can be played with a slide or with fingers to stop the notes. This style of guitar is played in the same manner as a standard guitar and is favored by blues musicians. The other category of resonator guitars have a thick square neck and are played on the musician’s lap. The strings are roughly 1 cm above the fretboard so it is only possible to play with a slide. Square neck resonator guitars are most often played by traditional and bluegrass musicians.

There is not much literature on resophonic instruments, with only brief mentions of them, but they have interesting properties which warrant further investigation [2]. In this study, a square neck inverted cone style resonator guitar is measured. Driving point admittance measurements are made using a hammer strike method to study the small signal response of the instrument. Resonator cones are made of very thin aluminum, typically less than 0.5 mm which is quite thin as compared to the standard top plate thickness of roughly 3 mm for traditional acoustic guitars. The cone of the guitar measured is 0.35 mm thick. Since the cones are thin, it is more likely that the instrument will exhibit nonlinear characteristics when played in normal conditions. To measure potential nonlinearities of the instrument, a modal shaker was used to drive the instrument with various amplitude sinusoidal sweeps.

*mrau@ccrma.stanford.edu

Mode fitting is performed on the small and large signal admittance measurements to be used as a body filter for a waveguide string synthesis model [3, 4, 5, 6, 7]. A modal architecture is used for this body filter so that the frequency, damping, and amplitude of each resonance can be adjusted during the synthesis. Some of the resonances observed with the shaker are shown to exhibit nonlinear weakening spring characteristics, resulting in a lowering of resonance frequency at high amplitude. These nonlinear resonances are approximated as time-varying linear modes using the modal architecture to vary the resonant frequency in relation to the amplitude of the bridge velocity at each mode. Synthesis examples are generated and compared to determine if this nonlinear behavior is audible and worth including in a model where a trade-off between accuracy and computational complexity has to be taken into account.

The outline is as follows. Section §2 describes the measurements of resonator guitar. Then in §3 we describe the modal analysis and how the parameters are obtained. The waveguide synthesis model is described in §4. The results are discussed in §5. Finally, in §6 concluding remarks are provided.

2 MEASUREMENTS

A square neck resonator guitar with a single inverted cone was measured as part of this study. Small signal driving point admittance measurements were made using a hammer strike method while large signal measurements were made with a modal shaker.

2.1 Measurement Setup

The guitar was suspended vertically by its tuning pegs and the bottom end pin was supported lightly with foam to insure the instrument remained mostly stationary. The strings were tuned to a common tuning of GBDGBD having frequencies 98.00, 123.47, 146.82, 196.00, 246.94, and 293.66 Hz. While the body resonances were being measured, all strings were damped using foam. A replacement bridge was manufactured for the instrument, as not to harm the original bridge when the shaker was attached. This bridge caused the low strings to be slightly offset from their normal position. The bridge was used for all measurements, including when the shaker was not used. The measurement setup is shown in Fig. 1.

2.2 Small Signal Measurements

Small signal bridge admittance measurements were taken by striking the bridge perpendicular to the instrument string's lengthwise direction. The miniature force hammer (PCB 086E80) was suspended as a swinging pendulum and dropped remotely. A Polytec PDV-100 laser Doppler vibrometer (LDV) was used to measure the resulting vibrations. The laser was focused as close as possible to the striking location of the hammer to measure the driving point velocity. The measured driving point force and velocity are used to compute the admittance in the frequency domain as $\Gamma(\omega) = V(\omega)/F(\omega)$, where V and F are the velocity and force, and ω is the frequency. Bridge admittance measurements were taken with the force hammer and vibrometer in the direction perpendicular to the top plate of the guitar. Measurements were also taken in the direction parallel to the top of the guitar and normal to the string, and with the hammer striking along this direction and the vibrometer measuring perpendicular to the top plate. These additional measurements allow for a two dimensional model which includes both directions of transverse string vibration to be constructed with coupling between the directions, but for simplicity, only a one dimensional string model was constructed at this time.

2.3 Large Signal Measurements

In order to check if the resonator guitar's modes exhibit nonlinear behavior, the instrument was driven with a signal having greater force. A modal shaker (Modal Shop 2004E) was used to drive the instrument. A force sensor (PCB 208C01) was used to measure the force imparted by the shaker. The LDV was again used to measure the resulting velocity of the instrument's vibrations. Epoxy was used to glue the shaker tip to the bridge of the guitar, ensuring that the shaker would stay attached as the instrument was driven. Twenty-second long

Figure 1. Measurement Setup showing the LDV, force hammer, and shaker. Note, the shaker's force sensor is not shown.

linear sinusoidal sweeps ranging from 50-2000 Hz were played through the shaker at thirteen different amplitude levels. Sine sweep measurements were made increasing from 50-2000 Hz, and decreasing from 2000-50 Hz to check if the resonant behavior included hysteresis.

3 MODAL ANALYSIS

The bridge admittance measurements are used to form efficient digital filters to be used in a waveguide synthesis model. Modal fitting is performed on the admittance measurements to form a parallel bank of second-order filters which simulate the instrument's vibrational characteristics.

3.1 Mode Fitting

Mode fitting was performed on the hammer and sweep bridge admittance measurements to gain insight into the resonant frequencies, damping, and amplitudes. Modes were fit assuming the system has damped harmonic oscillator behavior with an impulse response of the form,

$$h(t) = \sum_{m=1}^{M} \gamma_m e^{2\pi f_m t(i-\zeta_m)}, \tag{1}$$

where γ_m, f_m, and ζ_m are the amplitude, natural frequency, and damping ratios of modes $m = 1,2,...,M$ [8, 9]. The mode fitting was done using a method derived by Jonathan Abel which involves analysis of the eigenstructure of a Hankel matrix of admittance impulse response samples [10]. The M largest singular values of this decomposition can be viewed as the singular values associated with the signal space as opposed to the noise space, and thus M was used as the model order. This mode fitting architecture does not guarantee positive-real modes which are needed to ensure the stability of the filters. However, the measurements were of high enough quality that when properly processed, the fitting yielded positive-real modes. The complex amplitudes were ob-

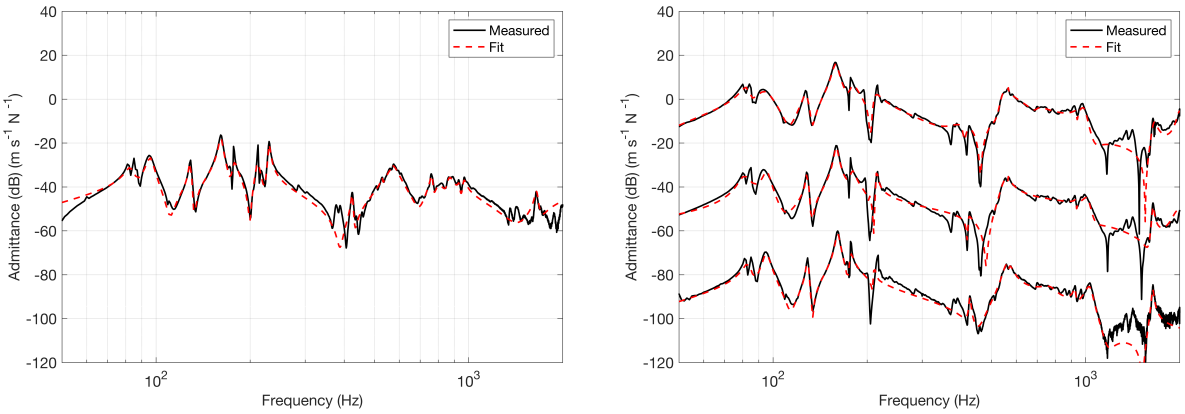

(a) Hammer Taps

(b) Shaker Sweeps

Figure 2. Figure 2a shows the measured and fit admittance from the hammer taps with M = 24 modes. Figure 2b Shows the measured and fit admittance from the shaker sweeps having RMS velocity of 0.000041, 0.0032, and 0.0102 m s^{-1} with M = 14, 16, and 18 modes respectively. The shaker sweeps are offset by -40, 0, and 40 dB for clarity.

tained using least squares to minimize the error between the measured admittance and a basis of the fit modes. Figure 2a shows the measured and fit admittance as measured with the hammer tap method.

3.2 Nonlinear Resonances

Figure 2b shows the measured and fit admittance as measured with the shaker sweep method at three different levels. The sweeps were made at different amplitudes, and since the waveguide model will be constructed to model transverse velocity and force waves, the sweep levels are characterized here by the root mean square (RMS) velocity of the measured velocity during the sweep.

Figure 3 shows a zoomed in version of the low frequency portion of the admittance measured using the shaker for 13 different amplitude levels of the upward frequency trajectory sweeps. Note that for some of the modes, the resonant frequency shifts to a lower frequency at higher amplitudes. This phenomenon is known as a weakening spring if the modes are approximated as a nonlinear spring system such as a Duffing oscillator [11, 12]. The downward frequency trajectory sweeps show similar behavior, and no hysteresis is observed, so only the upward trajectory sweeps are shown.

4 DIGITAL WAVEGUIDE MODEL

To simulate the resonator guitar, we use the digital waveguide architecture where samples stored in delaylines represent the transverse velocity waves of the simulated strings. The left and right travelling velocity waves are represented by $v^+(n)$ and $v^-(n)$, and the force waves are represented by $f^+(n)$ and $f^-(n)$ for each string. The transverse velocity and force at the bridge junction are $v(n) = v^+(n) + v^-(n)$ and $f(n) = f^+(n) + f^-(n)$. To calculate the reflected velocity waves at the bridge, the reflection scattering junction,

$$S_b(z) = \frac{R_B(z) - R_s}{R_B(z) + R_s}, \tag{2}$$

can be calculated from the string characteristic impedance, R_s, and the bridge impedance $R_B(z) = 1/\Gamma(z)$. The string impedance is calculated as, $R_s = \sqrt{T\varepsilon}$, where the tension, T, and the linear mass density, ε, of the string are calculated from manufacturer provided data [13]. The reflection scattering junction is implemented as a

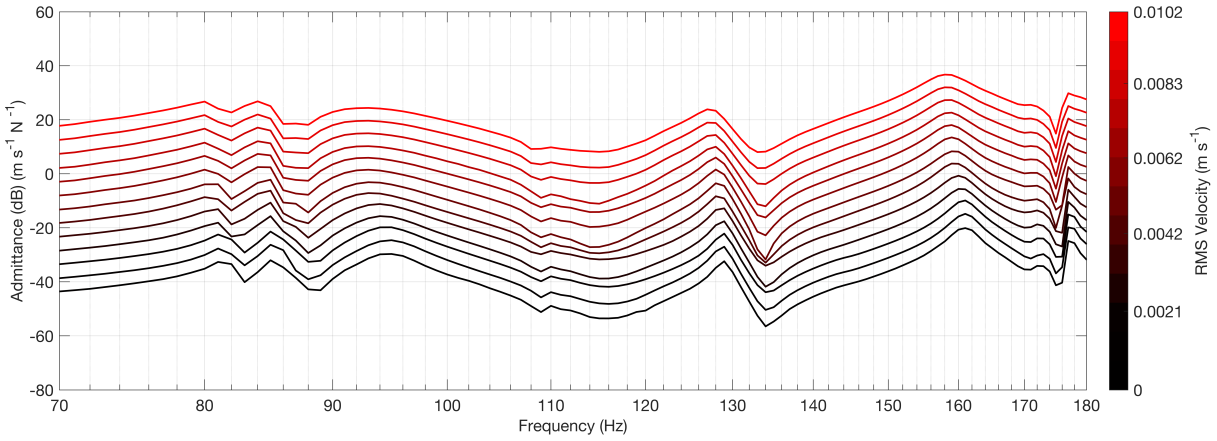

Figure 3. Admittance from the upward frequency trajectory shaker sweep measurements at 13 different levels. The 12 highest levels are offset in increments of 5 dB for clarity.

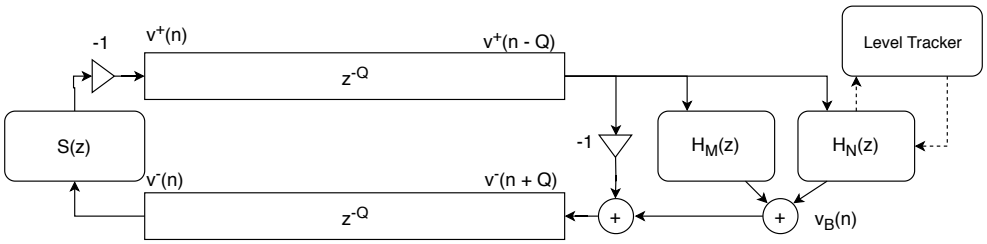

Figure 4. Block diagram of the waveguide synthesis architecture.

parallel bank of second order filters as in [7], and used to calculate the reflected transverse velocity samples at the bridge.

For simplicity, and since the resonance nonlinearity is the focus of this paper, only a 1D string with no string to string coupling is implemented. The neck termination is treated as a simple lossless reflection. The string losses are modeled in a simplified way using a 2nd order FIR lowpass filter, shown as $S(z)$. Two delay lines are used, one for $v^+(n)$ and one for $v^-(n)$. They are each of length $Q = \frac{f_s}{2f_0}$, where f_s is the sample rate and f_0 is the fundamental frequency of the string being simulated. At this time, the instrument radiation is not simulated, and the output is taken as the bridge velocity $v_B(n)$.

A block diagram of the waveguide synthesis is shown in Fig. 4, and the details of the bridge termination filter will be explained in the following two subsections.

4.1 Bridge Termination Filter Architecture

The bridge reflectance filter is constructed as a parallel bank of second order filters which can include linear and nonlinear resonances. The shaker admittance measurements were not as reliable as the hammer taps, so the hammer tap measurement modes are used as the basis for the reflectance filter bank. However, 5 distinct nonlinear resonances were found using the shaker sweep measurements, they are at 83.2, 95.7, 128.8, 161.1, and 177.5 Hz. These are likely not the only nonlinear resonances, but they were found with more confidence than other modes, so only this set will be modeled as nonlinear resonances while the rest are modeled as linear modes. This leaves $M = 19$ linear modes and $P = 5$ nonlinear resonances.

The filter banks are constructed in terms of their center frequency, damping ratio, and complex amplitude to give the two parallel filter banks as:

$$H_m(z) = \gamma_m \frac{1 - z^{-2}}{1 + a_{m,1} z^{-1} + a_{m,2} z^{-2}}, \tag{3}$$

$$H_p(z) = \gamma_p \frac{1 - z^{-2}}{1 + a_{p,1} z^{-1} + a_{p,2} z^{-2}}, \tag{4}$$

where $a_{m,1} = -2r_m \cos(2\pi f_m / f_s)$, and $a_{m,2} = r_m^2$, with $r_m = \exp(-2\pi f_m \zeta_m / f_s)$ being the pole radius, and f_s the sampling rate. The variables indexed with m represent the linear modes with $M = 19$ being used, and the variables indexed with p represent the nonlinear resonances with $P = 5$.

The nonlinear resonances are modeled as time-varying linear modes. As a first approximation, only the center frequency of the modes will be varied. The center frequencies and peak velocity of each of the nonlinear resonances were calculated at each RMS velocity level. To parameterize the nonlinear resonance frequency as a function of the instantaneous velocity, v_p, linear fits were made of the form, $f_p(v_p) = c_m \times v_p + f_m$, where f_p is the calculated nonlinear resonance center frequency, c_m is the slope of the fit, and f_m is the center frequency calculated from the hammer tap measurement. During the shaker measurements, the instrument was mass loaded by the force sensor, decreasing the center frequencies, so the center frequencies from the hammer measurements are used as the base frequencies for the nonlinear resonances. The parameters of the linear fitting are shown in Table 1.

Table 1. Center frequency and slope of the linear fitting to calculate the amplitude dependant nonlinear resonance center frequencies.

Center Frequency, f_m (Hz)	83.2	95.7	128.8	161.2	177.5
Frequency Slope, c_m (m^{-1})	-8.3	-12.6	-21.4	-16.7	-0.6

4.2 Level Tracking

To vary the center frequencies of the nonlinear resonances, an estimate of each mode's component of the bridge velocity, $v_n(n)$ was needed. The level detection is done on the output of each nonlinear resonance's associated filter using a leaky integrator based peak detector. This is implemented using the update equation,

$$\begin{aligned} &\text{if } |v_p(n)| > \lambda\text{:} \\ &\quad \lambda = \lambda + (1 - e^{\frac{-1}{\tau_a f_s}})(|v_p(n)| - \lambda) \\ &\text{else:} \\ &\quad \lambda = \lambda + (1 - e^{\frac{-1}{\tau_r f_s}})(|v_p(n)| - \lambda), \end{aligned} \tag{5}$$

where λ is the level estimate, $v_p(n)$ is the bridge velocity at each mode, τ_a is the time constant when the level detection is increasing, and τ_r is the time constant when it is decreasing. The attack and release time constants were chosen as $\tau_a = 0.1$ ms, and $\tau_1 = 100$ ms, so that transients are detected quickly but the level does not drop directly after the transients [14].

5 RESULTS AND DISCUSSION

String pluck approximations were generated by initializing the delaylines with a triangular string displacement which was used to calculate the transverse velocity at each sample of the delayline. Example plucks are generated using only linear modes and using the hybrid linear-nonlinear model. Audio examples can be found

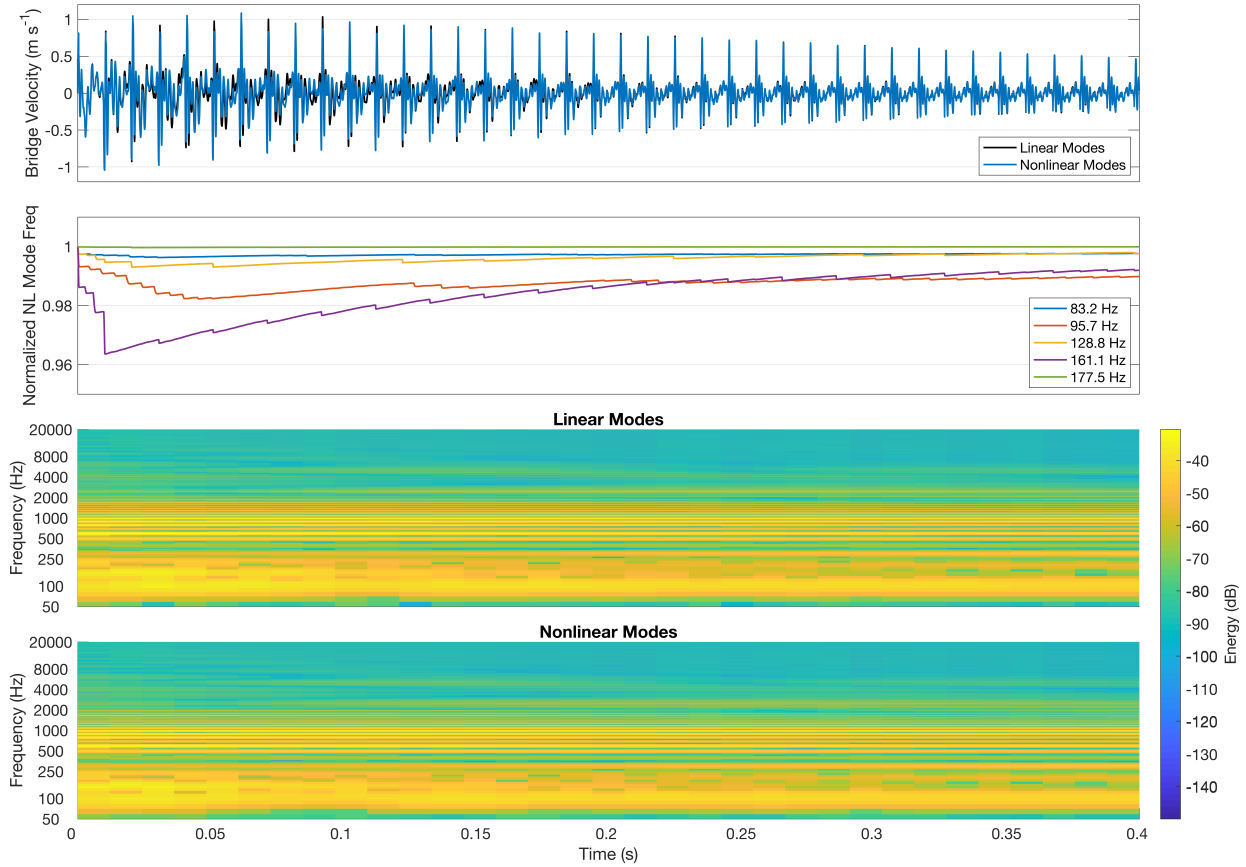

Figure 5. Bridge velocity and normalized frequencies of the nonlinear resonances during a one pluck of the low G string at 98 Hz. Spectrograms are shown, one with only linear modes, and one which included the nonlinear resonances.

online[1]. Figure 5 shows a linear and a nonlinear pluck as well as the normalized frequencies of the nonlinear resonances during the nonlinear pluck. It is clear that the waveforms are quite similar but deviate, especially when the bridge velocity is high.

Informal listening suggests that the linear and and nonlinear models are quite similar, but do have a slight timbre difference, especially during the attack of the plucks. However, this evaluation is informal and a formal listening test would be required to give more conclusive results of the timbre differences.

6 CONCLUSIONS

Measurements of a resonator guitar were made with small and large signal excitations as a basis for modal analysis. The small signal hammer excitation provided high quality measurements to perform modal fitting, while the large signal shaker measurements revealed that some of the instrument's resonances behave nonlinearly. These linear and nonlinear resonance parameters were used to create a digital waveguide model of the resonator guitar.

[1] https://ccrma.stanford.edu/~mrau/ISMA2019/

This study provides preliminary results which suggest that modeling the weakly nonlinear resonances of resonating instruments may be important to properly model the timbre, especially during transients. However, this study is not complete and there is plenty of room for future work. First, the model constructed is only one dimensional and does not include string-string coupling. Expanding on this model would likely aid in the accuracy. As well, the signals used to synthesize the pluck are not physical, as a higher energy pluck will not be an exactly scaled version of a low energy pluck. The model uses the bridge velocity as the output signal, but a more accurate model would include radiation modeling [7].

The nonlinear resonances were approximated as time-varying linear modes, but this assumption should be checked to see how well it perceptually compares to a more complicated model. A more complicated model may also include varying the damping ratios and complex amplitudes of each resonance.

In addition to improvement to the waveguide model, more measurements could be made to improve the modal fitting. More shaker sweeps could be made at other amplitude levels and on different days to confirm the results. As well, other similar instruments could be measured and modeled to see how this approach translates to similar or dissimilar instrument modeling.

REFERENCES

[1] Peter T. Veru, *The National-Dobro Guitar Company: How the resonator guitar survived the age of electric amplification*, The George Washington University, 2009.

[2] Thomas D. Rossing and Andrew Morrison, *The science of string instruments*, Springer, 2010.

[3] Julius O. Smith III, "Efficient synthesis of stringed musical instruments," in *Proc. of the International Computer Music Conference*, 1993, pp. 64–71.

[4] Matti Karjalainen, Vesa Välimäki, and Tero Tolonen, "Plucked-string models: From the Karplus-Strong algorithm to digital waveguides and beyond," *Computer Music Journal*, vol. 22, no. 3, pp. 17–32, 1998.

[5] Julius. O. Smith III, *Physical Audio Signal Processing*, W3K Publishing, 2004, online book: http://-ccrma.stanford.edu/~jos/pasp/.

[6] Esteban Maestre, Gary. P. Scavone, and Julius. O. Smith III, "Digital modeling of bridge driving-point admittances from measurements on violin-family instruments," in *Proc. of the Stockholm Music Acoustics Conference*, 2013, pp. 101–108.

[7] Esteban. Maestre, Gary. P. Scavone, and Julius. O. Smith III, "Digital modeling of string instrument bridge reflectance and body radiativity for sound synthesis by digital waveguides," in *Proc. of the IEEE Workshop on Applications of Signal Processing to Audio and Acoustics*. IEEE, 2015.

[8] Anders Brandt, *Noise and Vibration Analysis: Signal Analysis and Experimental Procedures*, John Wiley & Sons, 2011.

[9] Agilent Technologies, "Fundamentals of modal testing," 2000.

[10] Jonathan S. Abel, "Direct modal filter design," *Personal Communication*, November 2018.

[11] Lev Landau and Evgenii Lifshitz, *Course of theoretical physics: Mechanics*, vol. 1, Elsevier, 2013.

[12] Marco Amabili, *Nonlinear vibrations and stability of shells and plates*, Cambridge University Press, 2008.

[13] D'Addario, "Catalog Supplement/String Tension Specifications: A complete technical reference for fretted instrument string tensions," 2019.

[14] Udo Zölzer, *DAFX: Digital Audio Effects, 2nd Edition*, John Wiley & Sons Ltd, Hamburg, Germany, 2011.